Heavy quasiparticles in $CeCu_6$ studied using magnetic quantum oscillations

1990 J. Phys.: Condens. Matter 2 8123

(http://iopscience.iop.org/0953-8984/2/41/002)

J. Phys.: Condens. Matter **2** (1990) 8123–8136. Printed in the UK

Heavy quasiparticles in $CeCu_6$ studied using magnetic quantum oscillations

S Chapman†§, M Hunt†, P Meeson†, P H P Reinders†‖, M Springford† and M Norman‡

† H H Wills Physics Laboratory, University of Bristol, Tyndall Avenue, Bristol BS8 1TL, UK

‡ Argonne National Laboratory, Argonne, Illinois, USA

Received 6 April 1990

Abstract. Angle resolved measurements of the de Haas–van Alphen effect are reported in the heavy-fermion compound $CeCu_6$. The experiments confirm the presence at low temperature of a sharply defined Fermi surface resulting from the existence of heavy, long-lived, charged, fermion quasiparticles. LMTO electronic structure calculations have been performed within the local density approximation, in which the f electrons are included as either band or core states, but in neither case are the results in satisfactory agreement with experiment. The measured effective masses, which are in the range 6–80 m_e, are found to be magnetic field dependent in a manner which closely resembles that of the linear specific heat coefficient. We deduce that, in zero applied field, the mass renormalization in $CeCu_6$ is greater than 200.

1. Introduction

In recent years, a new branch of metal physics has come into prominence which is concerned with the unusual low temperature properties of certain ordered metallic compounds containing either rare-earth (normally Ce) or actinide (normally U) atoms. Whilst at high temperatures, $T \gg T_0$, where T_0 is a characteristic temperature usually in the range 1–10 K, such systems normally exhibit properties characteristic of an assembly of isolated magnetic ions, such as for example a Curie law dependence of magnetic susceptibility, at low temperatures, $T \ll T_0$, their transport and thermodynamic properties appear to be dominated by the presence of a Fermi liquid of very strongly renormalized quasiparticles, or heavy fermions. As evidence of this one may cite the abnormally high values of the linear coefficient of specific heat γ and temperature independent (Pauli) susceptibility χ, the existence at low temperatures of a strong T^2 component to the electrical resistance and a Korringa law dependence of the NMR spin–lattice relaxation, T_1T = constant. Whilst the existence of freely propagating heavy fermionic excitations with effective masses $\sim 10^2$–10^3 times greater than the free-electron

§ Present address: School of Mathematical and Physical Sciences, University of Sussex, Brighton, Sussex BN1 9QH, UK

‖ Present address: Institut für Festkörperphysik, Technische Hochshule Darmstadt, Fachbereich 5, Hochschulstrasse 8, 6100 Darmstadt, Federal Republic of Germany.

0953-8984/90/418123 + 14 $03.50

mass is itself most intriguing, perhaps even more so has been the discovery that in certain compounds superconducting pairs are formed from within the heavy electronic Fermi liquid. Given the unusual normal state properties there is the expectation that the superconductivity is also unconventional, and recent work on UPt_3 [1], for example, provides strong support for this view.

The present experiments were undertaken in an attempt to gain some understanding of the *normal* state of heavy fermion compounds by employing one of the most powerful experimental methods which may be used to study electron quasiparticles in metals, the de Haas–van Alphen (DHVA) effect. The first successful measurements were made in $CeCu_6$, and have been reported briefly by us elsewhere [2, 3]. Since then, experiments have been reported in a number of other compounds as follows; UPt_3 [4, 5, 6], CeB_6 [7, 8], $CeRu_2Si_2$ [6], $CeAl_2$ [3, 6, 9], CeNi [10, 11] and $CeCu_2Si_2$ [12].

Amongst the heavy fermions, $CeCu_6$ has one of the largest known electronic specific heat coefficients, $\gamma = 1.67\ \mathrm{J\,mol^{-1}\,K^{-2}}$ [13], from which it follows that an effective overall mass enhancement ratio of order 10^2—10^3 is anticipated. As discussed below, this has important consequences for the temperature range over which quantum oscillations may be studied. In common with $CeAl_3$, which is similarly enhanced, it shows neither magnetic order nor superconductivity, but remains paramagnetic, at least down to temperatures of 10 mK. Unlike $CeAl_3$, however, single crystals may readily be prepared, and partly for this reason $CeCu_6$ has been extensively studied. At low temperatures, with $\boldsymbol{B} \| \boldsymbol{c}$, χ has the value 0.07 emu $\mathrm{mol^{-1}}$ [13], whilst the resistivity shows a T^2-dependence below about 30 mK [14] with coefficient 71 $\mu\Omega$ cm $\mathrm{K^{-2}}$ for a c-axis sample.

Amato *et al* [13] have measured the thermodynamic and transport properties of single crystalline $CeCu_6$, in a magnetic field, and have identified low and high field regimes with a crossover field of ~4.5 T. They conjecture that, below this field, antiferromagnetic correlations dominate, whereas above, the system is in a highly (spin) polarized state. They find a strong anisotropy of the quenching of γ by magnetic fields, being a maximum for $\boldsymbol{B} \| \boldsymbol{c}$ and negligible (at 7.5 T) for $\boldsymbol{B} \| \boldsymbol{b}$. The same quenching has also been studied in polycrystalline samples by Stewart [15] in fields extending to 24 T.

The incipient magnetic order in $CeCu_6$ has been the subject of several investigations. In alloying experiments on $Ce(Cu_{1-x}Ag_x)_6$, Gangopadhyay *et al* [16] infer the presence of an antiferromagnetic ground state for $0.013 < x < 0.1$, from measurements of γ and χ. The neutron scattering experiments of Aeppli *et al* [17], whilst confirming the absence of magnetic order in pure single crystals, revealed the presence of short range antiferromagnetic correlations. Finally, the anisotropy of the magnetic excitation spectrum is considered by de Visser *et al* [18] to be responsible for the large anisotropy in the low temperature linear thermal expansion.

Our paper is organized as follows. We consider first the theory of magnetic quantum oscillations in heavy fermion systems, drawing heavily on recent work based on the periodic Anderson model. Experimental results are then presented in section 3 followed by the results of an LDA band structure calculation in section 4. Finally, in section 5, we discuss and summarize the conclusions of this investigation.

2. Theory of the DHVA effect in heavy fermion systems

There have been several attempts to derive a theory of the DHVA effect in heavy fermion and other strongly interacting Fermi systems. Assuming that they behave as Fermi liquids, Stamp [19] used a statistical quasiparticle approach to show that there are

deviations from the standard (semiclassical) theory [20] although he concludes that, with the exception of the mass renormalization, these will normally be small. Since, however, it is generally thought that mass enhancements arise from many-body interactions, in particular through hybridization between conduction electron and localized but highly correlated 4f and 5f electrons on the rare-earth site, an alternative starting point, which is rather closer to a microscopic description, is the periodic Anderson Hamiltonian, as employed by Rasul [21] and Wasserman *et al* [22]. Both these analyses find the mass enhancement occurring in the DHVA amplitude to be the same as that found in the specific heat, although only the latter includes magnetic field dependent effects, such as are observed in the present experiments. We quote here only the final result for the oscillatory free energy [22]

$$\Omega_{\rm osc} = C \sum_r \frac{(-1)^r}{r^{3/2}} K_r D_r \cos\theta_r \tag{1}$$

in which the interactions enter both the phase θ_r and the thermal damping K_r as follows,†

$$C = -[(eB/2\pi\hbar)^{3/2} k_{\rm B} T]/(2\pi)^{1/2} \tag{2}$$

$$\theta_r = 2\pi r F/B - \psi_r \tag{3}$$

$$\psi_r = g(m_{\rm B}/m_{\rm e})\pi r J(n_{\rm f}/N\rho_0 k_{\rm B} T_{\rm A} + 1) + \pi/4 \tag{4}$$

$$K_r = [\sinh(2\pi^2 r k_{\rm B} T/\hbar\omega_{\rm c}^*)]^{-1} \tag{5}$$

$$\omega_{\rm c}/\omega_{\rm c}^* = m^*/m_{\rm B} = 1 + 2Dn_{\rm f} k_{\rm B} T_{\rm A}/N(k_{\rm B} T_{\rm A} + Jh)^2 \tag{6}$$

and in which $m_{\rm B}$ is the band mass, $\omega_{\rm c} = eB/m_{\rm B}$, $\rho_0 = 1/2D$ is the density of conduction band states taken to be uniform in energy with 2D the conduction bandwidth, $n_{\rm f}$ the mean f-level occupation, N the degeneracy $(2J + 1)$, $T_{\rm A}$ a characteristic temperature and h is the reduced magnetic field, $h = g\mu_{\rm B}B$. The collision damping term $D_{\rm r}$ is presumed in the analysis to be unaffected by the renormalization,

$$D_{\rm r} = \exp(-r\pi/\omega_{\rm c}\tau) = \exp(-2\pi^2 r k_{\rm B} T_{\rm D}/\hbar\omega_{\rm c}) = \exp(-14.69 m_{\rm B} T_{\rm D}/B) \tag{7}$$

where τ is the quasiparticle lifetime and $T_{\rm D}$ the scattering (Dingle) temperature, although the product $m^* T_{\rm D}^*$ is often used in equation (7) where $m_{\rm B} T_{\rm D} = m^* T_{\rm D}^*$. For the approximations inherent in this approach and a description of the single channel approximation used to derive the above expressions, in which the dominant contribution to $\Omega_{\rm osc}$ comes from the level $m = -J$, the reader is referred to the original paper [22].

The occurrence of $\omega_{\rm c}^*$ in equation (5) has a profound effect on the amplitude of the magnetic oscillations. Whereas for ordinary metals, with $\omega_{\rm c}/\omega_{\rm c}^* = m^*/m_{\rm B} \approx m^*/m_{\rm e} \approx 1$, experiments are typically performed under the conditions, $T = 1$ K and $B = 10$ T, for which the amplitude factor $K_1 \approx 0.5$, in the case where $m^* = 100\, m_0$ the same experimental conditions yield $K_1 \approx 10^{-64}$! It is for this reason that quantum oscillation experiments in heavy fermion compounds must necessarily be performed at millikelvin temperatures. In weak fields such that $Jh \ll T_{\rm A}$, equation (6) yields the weak field enhancement of the magnetic susceptibility and specific heat in the mean field approximation [23]; $m^*/m_{\rm B} = 1 + 2Dn_{\rm f}/NT_{\rm A}$. This is also the result for the quasiparticle

† An error by a factor of 4 in the original paper [22] has been corrected in equation (2).

mass obtained by Rasul [21]. However, equation (6) explicitly anticipates a field dependence of the quasiparticle mass and, by implication, the specific heat coefficient γ. We shall return to this below.

3. Experimental details

As described elsewhere [2], the compound was first formed by melting under argon stoichiometric quantities of electropolished cerium and electrolytically purified copper in a water cooled copper boat. Subsequently, single crystals were grown by pulling from the melt in an RF heated tungsten crucible, also in an argon atmosphere. The samples used in the present experiment were cut from various regions of the boule and were found to have resistivities in the c-direction at 20 mK in the range 1.5–2.9 $\mu\Omega$ cm. $CeCu_6$ is orthorhombic at room temperature with four formula units per primitive cell. Close to 200 K it undergoes a structural phase transformation [24] from orthorhombic ($a = 8.109$, $b = 5.105$, $c = 10.159$, in Å) to a monoclinic structure ($a \rightarrow c' = 8.067$, $b \rightarrow a' = 5.080$, $c \rightarrow b' = 10.121$) but with little distortion as the angle $\gamma = 90°$ becomes $\beta = 91.36°$. Nevertheless, as a precaution, samples were cooled slowly through this region in order to minimize any deterioration. We shall use the orthorhombic notation throughout this paper.

The experiments were performed on samples immersed in the ^{3}He–^{4}He mixture in the mixing chamber of a top-loading dilution refrigerator, described elsewhere [25], in fields up to 14.5 T using the field modulation method at frequencies of between 1 and 18 Hz chosen to avoid sample heating. The sample could be rotated about an axis normal to $\boldsymbol{B}$ by means of a fibreglass rod passing directly into the mixing chamber. The temperature range used was 17–250 mK as measured using RuO_2 film resistors and a calibrated Ge thermometer situated in the zero field region in the extended mixing chamber.

A number of DHVA frequencies are seen, some of which are clearly harmonically related. By rotating the sample *in situ* about a known axis, this angle resolved DHVA spectrum in figure 1 was measured. The following features are noted.

(i) The lowest frequency branch has a value close to 120 T over much of the rotation diagram and is rich in harmonics.

(ii) Whether because of inferior crystal quality, or for intrinsic reasons related to the nature of the Fermi surface or high quasiparticle masses, the highest frequency observed was ~2600 T, corresponding to only 26% of the Brillouin zone cross section.

(iii) As indicated by the middle range of frequencies, $200\ \text{T} \leqslant F \leqslant 1000\ \text{T}$, the Fermi surface is evidently rather complicated and the topology of some of the branches is difficult to discern.

(iv) The dearth of signals for $\boldsymbol{B} \| \boldsymbol{b}$ is striking.

It follows from the summary of the theoretical analysis above, that the renormalized cyclotron effective masses may be determined in the usual way [20], from the temperature dependence of the amplitude of the quantum oscillations; namely by fitting the experimentally measured amplitudes to the function, $X_r/\sinh X_r$, in which $X_r = 2\pi^2 r k_B T/\hbar\omega_c^*$, in order to determine X_r and hence, knowing B, m^*. Implicit in this analysis is the assumption that the quasiparticle scattering, as expressed by equation (7), is independent of temperature. The results of this analysis are summarized in table

Table 1. Quasiparticle effective masses, m^*/m_e, in $CeCu_6$ determined from the temperature dependence of the amplitude of magnetic oscillations of frequency F. In the upper part of the table, only the approximate field range over which measurements were made is indicated. In the lower part of the table the exact mean field of each measurement is given. The units of F and B are tesla and of the quasiparticle velocity, $\langle v^* \rangle$, are m s^{-1}.

	F	B	m^*/m_e	$\langle v^* \rangle$
c-axis	2000	10–13	80	3.6×10^3
	1300	10–13	24	9.6×10^3
	1034	10–13	40	5.1×10^3
	740	10–13	23	7.5×10^3
	638	10–13	14	1.2×10^4
	122	6–10	6	1.2×10^4
	40	6–10	11	3.7×10^3
a-axis	758	10–13	57	3.1×10^3
	275	6–10	20	5.4×10^3
b-axis	114	6–10	8.5	8.0×10^3
c-axis	122	4.1	10.8 ± 1	
		4.6	8.6 ± 1	
		5.7	7.8 ± 0.5	
		10.6	6.0 ± 0.5	
	1034	10.3	34.6 ± 1	
		11.3	31.9 ± 1	
		12.2	29.6 ± 1	
a-axis	275	7.0	16.7 ± 2	
		10.35	17.0 ± 2	
		11.9	20.8 ± 2	

1. A search early on in this work for a magnetic field dependence of the masses gave a null result to within the experimental uncertainty [2]. Prompted, however, by the observation of an anisotropic field dependence of γ [13], a further search was made with greater experimental resolution. These results, which are also summarized in table 1, do reveal a field dependence for $\boldsymbol{B}$ directed along the c-axis, a result that we shall return to in the discussion in section 5 below. For this reason, the results in the upper part of table 1 are field averaged values as indicated.

4. Band structure calculation

In an attempt to interpret the DHVA frequencies in figure 1, linearized muffin-tin orbital (LMTO) band structure calculations [26], within the local density approximation (LDA), were performed, using the exchange–correlation potential of Hedin and Lundqvist [27]. As the low temperature monoclinic distortion is weak, the lattice used was that of the high temperature orthorhombic phase in order to gain some symmetry in the calculations, with atomic positions taken from the work of Vrtis *et al* [28]. Calculations were done both in the standard atomic sphere approximation (ASA) and including

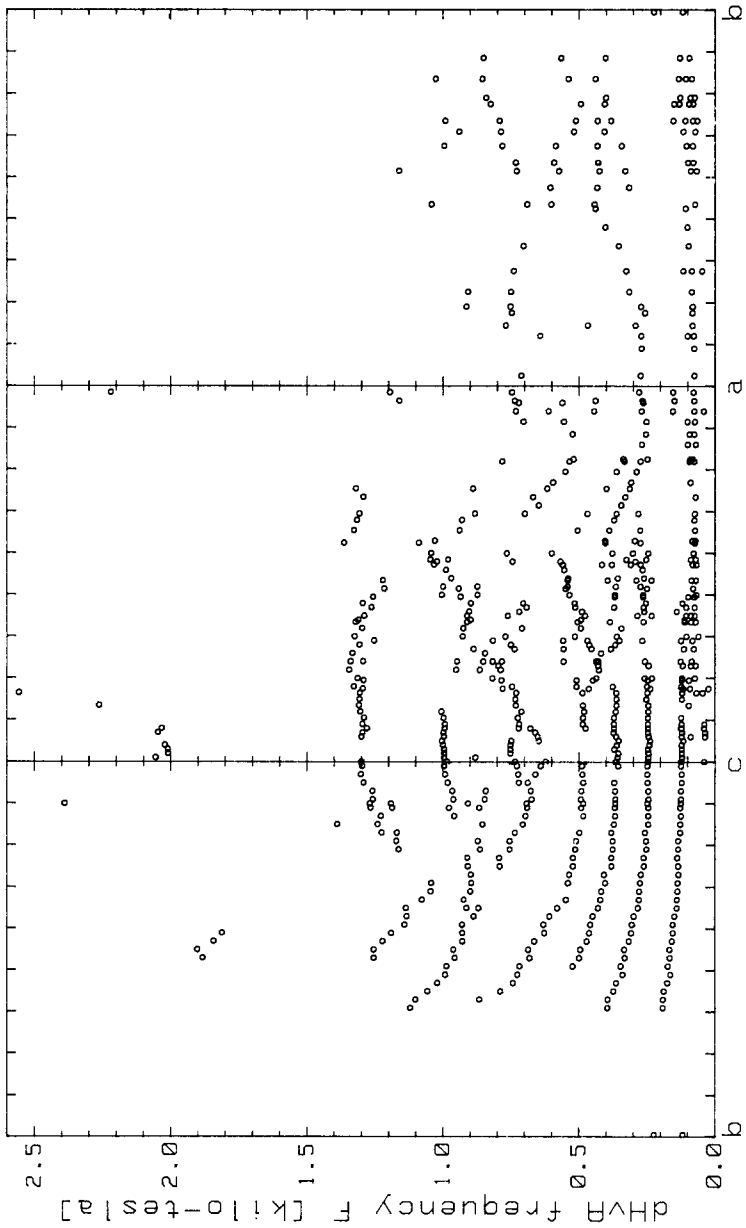

Figure 1. Orientation dependence of the measured DHVA frequencies in $CeCu_6$ in the principal planes. The orthorhombic notation is used.

combined correction (CC) terms, which take into account the overlap of the Wigner–Seitz spheres. Basis functions up to $l = 3$ were kept on the Ce sites, and up to $l = 2$ on the Cu sites. Calculations were also done including the f electrons as either band or core states. In the band case, the f electrons are treated in the same way as other valence states. This procedure works well for the heavy electron superconductor UPt_3 [29] and for the 'pudgy' electron metal $CeSn_3$ [30]. In the core case, the f electron is treated as an atomic state and was done in two different ways, one including $l = 3$ basis functions in the band states on the Ce sites, and the other not. This procedure works well for such cerium alloys as CeSb [31], CeB_6 [32] and $CeAl_2$ [3]. During the self-consistent cycles, a mesh of 18 k-points in the irreducible (1/8th) wedge was used to construct the charge densities. At the end of the cycles, it was necessary to generate eigenvalues at 175 k-points to obtain the Fermi surface to moderate precision, the Fermi surface being generated by performing a Fourier series spline fit to the eigenvalues. Only scalar relativistic effects were included (i.e. no spin–orbit) because of computational expense, although a fully relativistic calculation was done in the f-band case on a cruder 104 k-point mesh.

The basic results of these calculations are as follows. All cases had a Fermi surface composed of four bands which were topologically complicated and sensitive to changes of Fermi energy as small as 1 mRyd. The topology differs considerably between the f-band and the f-core cases. The topology was very sensitive to whether combined correction terms were included or not (unlike the case of UPt_3 [29]). The topology of the f-core case was also somewhat sensitive to whether $l = 3$ basis functions were included on the cerium sites or not. There appears to be less sensitivity to spin–orbit effects, as determined when comparing the scalar and fully relativistic calculations for the f-band calculation, although it should be remembered tht the fully relativistic surface was generated on a cruder mesh. These results tend to indicate that the LMTO procedure may not be adequate to accurately obtain the Fermi surface due to shape approximations to the potential and basis function limitations. These problems arise due to the low symmetry of the system combined with the complicated nature of the bands in the vicinity of the Fermi energy. This conjecture could be explored by performing linearized augmented plane wave (LAPW) calculations, but the latter may be prohibitively expensive from a computational standpoint.

Given the above caveats, the primary results for the f-band and f-core LMTO–CC calculations are shown in figures 2–5. They include plots of the Fermi surface in various symmetry planes and plots of the extremal areas versus field orientation in the c–a plane. Comparison with the experimental data for either case does not look promising. In particular, the tube-like structures seen in both calculations do not appear to be present in the experiments (these tubes lead to divergent extremal areas as one approaches a symmetry axis, as can be seen in figures 3 and 5). Whether this is due to possible inadequacies in the LMTO procedure for this metal as discussed above, or whether this is connected to a failure of the LDA as predicted for some cerium heavy fermion systems by Zwicknagl [33], remains to be seen. An interesting test is to compare the f-core results to the experimental DHVA results on $LaCu_6$ by Onuki *et al* [34]. The comparison indicates that, most likely, Onuki *et al* have missed quite a lot of the Fermi surface, although both theory and experiment do find 'tubes' along the c-axis. More detailed experiments on $LaCu_6$ (with the relevant band structure calculations) would be helpful in testing how adequate the LMTO calculations are for the non-f analogue metal. Until this question is resolved, it would be premature to conclude that the LDA 'fails' for the case of $CeCu_6$.

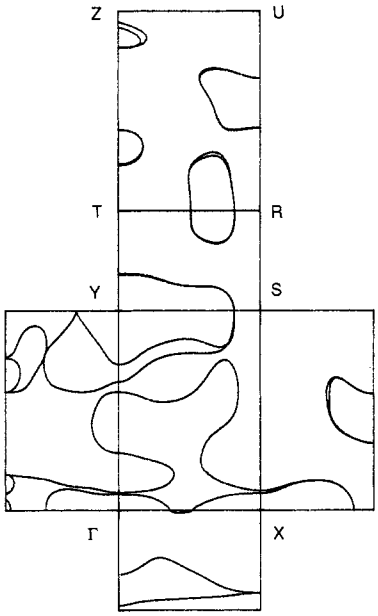

Figure 2. Plot of the LMTO-CC Fermi surface for the f-band case in various symmetry planes.

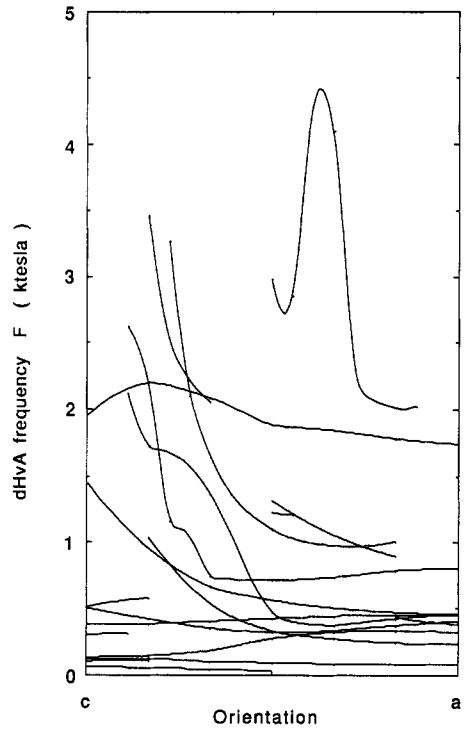

Figure 3. Plot of the LMTO-CC f-band extremal areas versus applied field direction from the *c*-axis (90) to the *a*-axis (0). Areas are in units of kilotesla.

Evidently, however, this is a possibility, and if true, then it could be the first known metal where this occurs.

5. Discussion

5.1. Quasiparticle masses

We turn our attention now to the quasiparticle masses in table 1. Even though the measurements in the upper part of the table are field averaged values, it is clear even so, from a comparison with similar measurements in $LaCu_6$ by Onuki *et al* [35] where m^* was in the range 0.1 to $1m_0$, that in $CeCu_6$, *all* orbits have strongly enhanced masses. That is, we find no evidence for the coexistence of heavy and light carriers. Interpreting the measured masses in the normal way in terms of the 'local' values of quasiparticle velocity.

$$m^* = \frac{\hbar}{2\pi} \oint \frac{\mathrm{d}\boldsymbol{k}}{\boldsymbol{v}_\perp^*} \tag{8}$$

in which $\boldsymbol{v}_\perp^*$ is the projection of $\boldsymbol{v}^*$ in the plane perpendicular to $\boldsymbol{B}$, we may then obtain

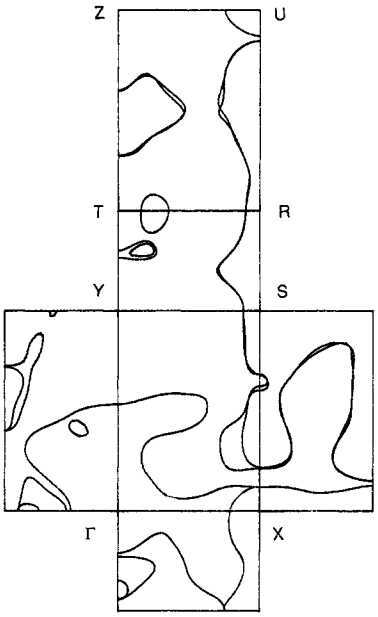

Figure 4. Plot of the LMTO-CC Fermi surface for the f-core case in various symmetry planes. The f-core calculation included $l = 3$ basis functions for the band states.

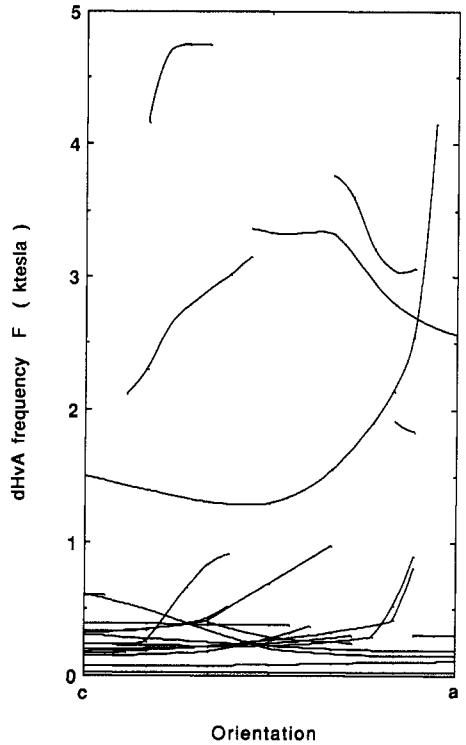

Figure 5. Plot of the LMTO-CC f-core extremal areas versus applied field direction from the *c*-axis (90) to the *a*-axis (0). Areas are in units of kilotesla.

an average value for the velocity, $\langle v^* \rangle$, around a particular orbit, in terms of the 'equivalent circular orbit radius', k_r, from the relation,

$$\langle v^* \rangle = \hbar k_r / m^* \qquad \text{where } \pi k_r^2 = 2\pi e F/\hbar. \tag{9}$$

The quasiparticle velocities estimated in this way are given in table 1, from which it is evident, as has been stressed elsewhere [2], that heavy fermions are slow fermions.

Of particular interest are the mass measurements at several different magnetic fields shown in the lower part of table 1, which we wish to compare with the specific heat measurements of Amato *et al* [13]. The latter revealed a considerable anisotropy in the field dependence of the quenching of γ and, for the *c*-axis, are represented by the solid line in figure 6, where they have been normalized to the zero-field value of $\gamma(0) = 1.67$ J mol^{-1} K^{-2}. For comparison, the quasiparticle masses must be normalized to their zero-field value, $m^*(0)$, a parameter which cannot of course be measured directly in the present experiments. However, an estimate may be obtained from the above theory, by first rewriting equation (6) in the form,

$$\left(\frac{m^*}{m_e} - \frac{m_B}{m_e}\right)^{-1/2} = \left(\frac{m^*(0)}{m_e} - \frac{m_B}{m_e}\right)^{-1/2} (1 + Jh/k_B T_A) \tag{10}$$

which, assuming that $m^*/m_B \gg 1$, for all fields of interest, simplifies to

$$(m^*/m_e)^{-1/2} = (m^*(0)/m_e)^{-1/2} (1 + Jh/k_B T_A). \tag{11}$$

Table 2. Estimates of the quasiparticle masses at zero magnetic field, corresponding to two DHVA frequencies measured in the *c*-direction, $F = 120$ T and 1034 T. The results in columns I and II were obtained by analysing the field dependence of the quasiparticle mass (table 1) using equation (11). In deriving T_A/g, in which T_A is the 'Kondo' temperature [22], it was assumed that crystalline electric fields reduce J, from its value of 5/2 corresponding to Ce^{3+} to $J = 1/2$ in the crystalline environment of $CeCu_6$ [36, 37]. In column III are given the values of the zero-field masses that bring the measured field variation of $m^*/m^*(0)$ into best agreement with that of $\gamma/\gamma(0)$ [13] by the method of least squares.

	I	II	III
F(T)	$m^*(0)/m_e$	T_A/g	$m^*(0)/m_e$
120	14	6.6	20
1034	113	4.3	120

Fitting this expression by linear regression to the measured values of m^*/m_e versus B in table 1, we obtain the results in columns I and II of table 2. We note that a value of $J = 1/2$ and g in the range 1–2 yields a value for T_A close to the 'Kondo' temperature of ~4 K normally attributed to $CeCu_6$ [36].

In the final column, III, of table 2 are given the values of the zero-field masses that bring the field variation of $m^*/m^*(0)$ into best agreement with that of $\gamma/\gamma(0)$, by the method of least squares. They are in reasonable agreement with the values in column I. These results for the quenching of the quasiparticle masses for the field in the *c*-direction are then superimposed on the equivalent data for the specific heat in figure 6, where the agreement is striking. Finally, we note the additional result shown in table 1 that, for the magnetic field directed along the *a*-axis, the mass is seen to be almost constant to within the experimental error. (There is perhaps an indication of a slight increase in mass at the highest field of 11.9 T). At this orientation, Amato *et al* [13] also observed γ to be independent of magnetic field, up to 7.5 T. We believe that this overall agreement between the present experimental results on the field dependence of the quasiparticle masses and the electronic specific heat coefficient gives strong support to a Fermi liquid description of $CeCu_6$ at low temperatures. We note too that if the results shown in figure 6 for two different orbits are representative of the behaviour of quasiparticles more generally over the Fermi surface, then we may conclude that the quenching of the mass by a magnetic field proceeds with a single characteristic energy; that is, it is independent of the particular orbit or quasiparticle mass. From this it follows that all quasiparticles are equally enhanced at zero magnetic field, consistent with our observation previously of the absence of any 'light' carriers, so that we may take the value of $\gamma(0)$ to be a measure of the enhancement. Furthermore, a comparison of the measured value of $\gamma(0) = 1.67$ J mol^{-1} K^{-2} [13] in $CeCu_6$ with the value 8 mJ mol^{-1} K^{-2} [37] in the f-electron free 'reference' compound, $LaCu_6$, yields

$$\gamma(CeCu_6)/\gamma(LaCu_6) = 210 \tag{12}$$

which we may take to be an approximate measure of the zero-field mass enhancement in $CeCu_6$ arising from electron–electron effects. The full renormalization of the band masses, which also includes electron–phonon effects will therefore be somewhat greater than this. It seems remarkable that such large renormalizations can occur at all, without giving rise to magnetic order, superconductivity or localization.

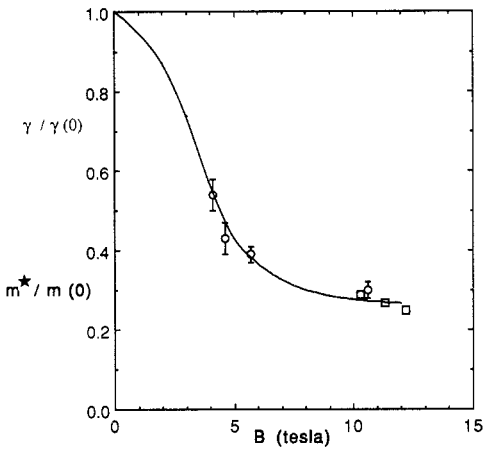

Figure 6. Variation with field of the quasiparticle mass, $m^*/m(0)$, for the two orbits, $F = 120$ T (○), and $F = 1034$ T (□) in $CeCu_6$. The solid line refers to the variation of the linear coefficient of specific heat, $\gamma/\gamma(0)$, as determined by Amato *et al* [13]. Both sets of measurements are for the magnetic field directed along the *c*-axis.

It is now possible to make an estimate of the density of quasiparticle states seen in these experiments for comparison with the specific heat measurements. Writing

$$\gamma(0) = 1.67 = (\pi^2/3)k_B^2 g(E_F) \tag{13}$$

we then obtain for the density of states in zero field, $g(E_F) = 2.67 \times 10^{45}$ states $\text{mol}^{-1}\,\text{J}^{-1}$. However, confining our attention to the *c*-direction we note that the quasiparticle masses in table 1 were mostly determined at magnetic fields in the range 10–13 T for which, from figure 6, γ has fallen to ~0.25 of its zero-field value. (The lowest frequency of 120 T was measured at a rather lower mean field but, as we shall see, it contributes negligibly to the density of states.) At these fields we then deduce from the specific heat that

$$g(E_F) = 6.66 \times 10^{44} \text{ states mol}^{-1}\,\text{J}^{-1} = 1.05 \times 10^{49} \text{ states m}^{-3}\,\text{J}^{-1} \tag{14}$$

in which we have assumed the orthorhombic unit cell containing four molecular units to derive the second value in equation (14).

In the absence of a detailed knowledge of the Fermi surface geometry and quasiparticle mass variation over it, we may only estimate the density of states from the DHVA experiments. Writing

$$g(E_F) = \frac{1}{4\pi^3}\int_S \frac{dS}{\hbar|v^*|} = \frac{1}{4\pi^3\hbar}\sum_i \frac{S_i}{v_i^*} \tag{15}$$

we have assumed in the second equation that the Fermi surface may be modelled by i spherical sheets, with surface areas, $S_i = 4\pi k_{F,i}^2$. Together with equation (9) we then obtain

$$g(E_F) = \frac{m_e}{\pi^2\hbar^2}\left(\frac{2e}{\hbar}\right)^{1/2}\sum_i \frac{F_i^{1/2} m_i^*}{m_e} = 4.58 \times 10^{44}\sum_i F_i^{1/2}(m_i^*/m_e) \text{ states m}^{-3}\,\text{J}^{-1}. \tag{16}$$

Substitution of the values of F_i and m_i^*/m_e from table 1 for the *c*-direction yields for the density of states

$$g(E_F) = 3.13 \times 10^{48} \text{ states m}^{-3}\,\text{J}^{-1} \tag{17}$$

a value that is only 30% of the value in equation (14), deduced from the specific heat.

We conclude from this that a substantial part of the Fermi surface, corresponding to even heavier quasiparticles than are recorded in table 1, remains unseen in the present experiments.

5.2. *Quasiparticle scattering*

From the field dependence of the amplitude of the magnetic oscillations, it is possible to derive a value for the quasiparticle scattering rate [20], although the analysis is complicated in the present case by the field dependence of the masses. We first generalize equation (2) to the case of an arbitrary shaped Fermi surface.

$$C_a = -[(eB/2\pi\hbar)^{3/2} k_B T]/|A''|^{1/2} \tag{18}$$

in which $|A''|$ is the familiar curvature factor having the value 2π for a sphere. The voltage, $V(t)$, detected in a coil surrounding the sample consists of a series of harmonics of the modulation frequency ω

$$V(t) = \sum_n V_n \sin(n\omega t) \tag{19}$$

from which the second harmonics, $n = 2$, was selected for study in the present experiment

$$V_2 = \sum_r A_r \cos(\theta_r) \tag{20}$$

with θ_r given by equation (3). The amplitude A_r contains the essential damping information contained in equations (5) and (7).

$$A_r = B_r r^{-1/2} K_r D_r \tag{21}$$

with B_r given by

$$B_r = C_a 16\pi\omega\varphi v J_2(r\alpha) B^{-2} F = 2.6093\omega\varphi v J_2(r\alpha) T B^{-1/2} F/2|A''|^{1/2}. \tag{22}$$

In this equation, φ is the sensitivity of the detection coil, v is the sample volume and J_2 is a second order Bessel function whose argument $r\alpha = 2\pi h_0 rF/B^2$, where $h_0 \cos \omega t$ is the modulation field. Consistent with using the single channel approximation, we note that B_r derived here is smaller by a factor 1/2 than that derived according to the LK theory [20]. Restricting our attention to the fundamental ($r = 1$) component of the quantum oscillations, it follows from the above analysis that a plot of

$$\ln(Amp) = \ln(A_1 B^{1/2}/J_2(\alpha) K_1 T) \tag{23}$$

versus B^{-1} should yield a straight line with gradient $(-14.69 m_B T_D)$ and intercept $(2.6093\omega\varphi v F/2|A''|^{1/2})$. Plots for the two frequencies, $F = 1034$ and 120 T, observed with $\boldsymbol{B}$ directed along the c-axis, are shown in figure 7. In evaluating K_1 in equation (23), the field dependence of quasiparticle mass is taken into account using equation (11), with the numerical values of the parameters given in columns I and II of table 2. Also shown is the calculated intercept corresponding to the 'infinite field amplitude' for which we used a spherical approximation for A'', as suggested by the rather isotropic rotation diagram for these two frequencies (figure 1). As seen in figure 7, the calculated intercept lies below the Dingle plot by a factor of ~5 and ~400 for the lower and higher frequencies respectively. Whilst for the lower frequency this difference might be attributed to experimental uncertainties, this cannot be the case for the higher frequency.

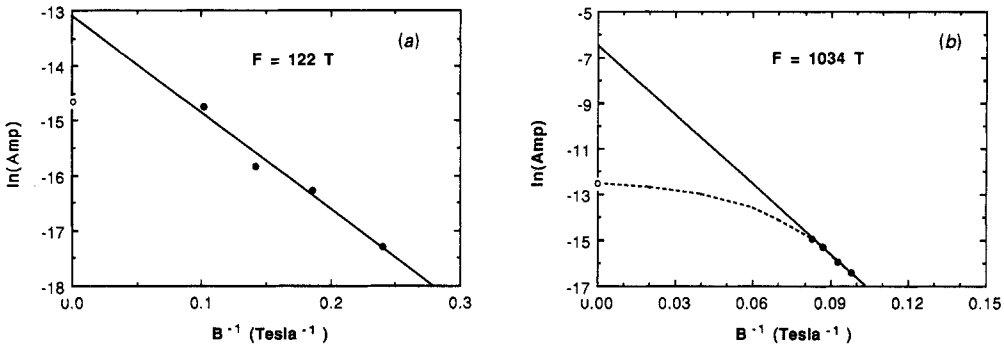

Figure 7. Dingle plots (see expression (23)) for $\boldsymbol{B}\|\boldsymbol{c}$ for the two frequencies (*a*) $F = 120$ T and (*b*) $F = 1034$ T. The variation of quasiparticle mass with field is included in the ordinate as explained in the text. The calculated intercept at infinite field is indicated by an open circle and is seen to lie below the intercept determined from the Dingle plot (solid line) which, for the case of the higher frequency in (*b*) where the discrepancy is ~400, is interpreted as indicating a field dependence of the quasiparticle scattering rate, as indicated schematically by the broken line.

We have considered several possible explanations of this discrepancy but firstly, we note that it is not significantly altered by analysing the data according to the LK theory. That the behaviour illustrated in figure 7(*b*) has been observed in several samples suggests that it is an intrinsic property of $CeCu_6$ and is unlikely to be a phase smearing phenomenon associated with sample imperfections. We are therefore inclined to the view that the theory outlined above is inadequate in some important respect. We propose that the discrepancy most probably has its origin in a breakdown of equation (7) which, whilst well established for non-magnetic impurity scattering in more normal metals [39], may well be an inadequate description of the scattering of such strongly renormalized quasiparticles. In particular, figure 7 may be interpreted as indicating a field dependence of the quasiparticle scattering rate, as indicated schematically by the broken line in figure 7(*b*). In this case, the 'slope' of the Dingle plot has no simple physical interpretation.

To test this hypothesis, we require a measure of the scattering rate at a particular value of the magnetic field. We note that this is provided by measurements of the relative amplitudes and phases of several DHVA harmonics, and that such experiments also yield information on the differential scattering between up- and down-spin quasiparticles [40]. We hope to report on such experiments at a later date.

Acknowledgments

This work is supported by the Science and Engineering Research Council by grants GR/E43829 and GR/E44031, and by the US Department of Energy, Office of Basic Energy Sciences, under Contract No W-31-109-ENG-38, and a grant of computer time at the Energy Research Cray-2 at the Magnetic Fusion Energy Computing Center. MN is indebted to Tamio Oguchi and Arthur Freeman for providing the LMTO codes that were used to perform these calculations, and to Dale Koelling for providing the spline fit and Fermi surface orbit tracer codes.

References

[1] Hasselbach K, Taillefer L and Flouquet J 1989 *Phys. Rev. Lett.* **63** 93
[2] Reinders P H P, Springford M, Coleridge P T, Boulet R and Ravot D 1986 *Phys. Rev. Lett.* **57** 1631; 1987 *J. Magn. Magn. Mater.* **63** & **64** 297
[3] Springford M and Reinders P H P 1988 *J. Magn. Magn. Mater.* **76** & **77** 11
[4] Taillefer L, Newbury R, Lonzarich G G, Fisk Z and Smith J L 1986 *J. Magn. Magn. Mater.* **63** & **64** 372
[5] Taillefer L and Lonzarich G G 1988 *Phys. Rev. Lett.* **60** 1570
[6] Lonzarich G G 1988 *J. Magn. Magn. Mater.* **76** & **77** 1
[7] Joss W, van Ruitenbeek J M, Crabree G W, Tholence J L, van Deursen A P J and Fisk Z 1987 *Phys. Rev. Lett.* **59** 1609; 1989 *J. Appl. Phys.* **63** 3893
[8] Onuki Y, Komatsubara T, Reinders P H P and Springford M 1989 *J. Phys. Soc. Japan* **58** 3698
[9] Reinders P H P and Springford M 1989 *J. Magn. Magn. Mater.* **79** 295
[10] Onuki Y, Kurosawa Y, Maezawa K, Umehara I, Isikawa Y and Sato K 1989 *J. Phys. Soc. Japan* **58** 3705
[11] King C A, Marshall A and Lonzarich G G 1989 *Physica B* at press
[12] Hunt M, Meeson P, Probst P-A, Reinders P, Springford M, Assmus W and Sun W 1990 *J. Phys.: Condens. Matter* **2** 6859
[13] Amato A, Jaccard D, Flouquet J, Lapierre F, Tholence J L, Fisher R A, Lacy S E, Olsen J A and Phillips N E 1987 *J. Low Temp. Phys.* **68** 371
[14] Sato H, Zhao J, Pratt W P, Onuki Y and Komatsubara T 1987 *Phys. Rev.* B **36** 8841
[15] Stewart G R, Andraka B, Quitmann C, Treadway B, Shapira Y and McNiff E J 1988 *Phys. Rev.* B **37** 3344
[16] Gangopadhyay A K, Schilling J S, Schuberth E, Gutsmiedl P, Gross F and Andres K 1988 *Phys. Rev.* B **38** 2603
[17] Aeppli G, Yoshizawa H, Endoh Y, Bucher E, Hufnagl J, Onuki Y and Komatsubara T 1986 *Phys. Rev. Lett.* **57** 122
[18] de Visser A, Lacerda A, Haen P, Flouquet J, Kayzel F E and Franse J J M 1989 *Phys. Rev.* B **39** 11301
[19] Stamp P C E 1987 *Europhys. Lett.* **4**(4) 453
[20] See, for example,
Shoenberg D 1984 *Magnetic Oscillations in Metals* (Cambridge: Cambridge University Press)
[21] Rasul J W 1989 *Phys. Rev.* B **39** 663
[22] Wasserman A, Springford M and Hewson A C 1989 *J. Phys.: Condens. Matter* **1** 2669
[23] Newns D M and Read N 1987 *Adv. Phys.* **36** 799
[24] Asano H, Umino M, Onuki Y, Komatsubara T, Izumi F and Watanabe N 1986 *J. Phys. Soc. Japan* **55** 454
[25] Reinders P H P, Springford M, Hilton P, Kerley N and Killoran N 1987 *Cryogenics* **27** 689
[26] Andersen O K 1975 *Phys. Rev.* B **12** 3060
[27] Hedin L and Lundqvist B I 1971 *J. Phys. C: Solid State Phys.* **4** 2064
[28] Vrtis M L, Jorgensen J D and Hinks D G 1986 *Physica* B **136** 489
[29] Wang C S, Norman M R, Albers R C, Boring A M, Pickett W E, Krakauer H and Christensen N E 1987 *Phys. Rev.* B **35** 7260
Norman M R, Albers R C, Boring A M and Christensen N E 1989 *Solid State Commun.* **68** 245
[30] Koelling D D 1982 *Solid State Commun.* **43** 247
[31] Norman M R and Koelling D D 1986 *Phys. Rev.* B **33** 6730
[32] Norman M R and Min B I 1989 unpublished
[33] Zwicknagl G 1988 *J. Magn. Magn. Mater.* **76** & **77** 16
[34] Onuki Y, Umezawa A, Kwok W K, Grabtree G W, Nishihara M, Komatsubara T, Maezawa K and Wakabayashi S 1987 *Japan. J. Appl. Phys. Suppl.* 3 (LT18) **26** 509
[35] Onuki Y, Nishihara M, Fujimura Y and Komatsubara T 1986 *J. Phys. Soc. Japan* **55** 21
[36] Onuki Y and Komatsubara T 1987 *J. Magn. Magn. Mater.* **63** & **64** 281
[37] Zemlrli S and Barbara B 1985 *Solid State Commun.* **56** 385
[38] Sumiyama A, Oda Y, Nagano H, Onuki Y and Komatsubara T 1985 *J. Phys. Soc. Japan* **54** 877
[39] Springford M (ed) 1980 *Electrons at the Fermi Surface* (Cambridge: Cambridge University Press) chs 8, 9
[40] Reinders P H P, Springford M, Boulet R and Coleridge P T 1987 *Japan. J. Appl. Phys. Suppl. 3* (LT18) **26** 505